Temperature-independent rescaling of the local activation barrier drives free surface nanoconfinement effects on segmental-scale translational dynamics near Tg

Daniel Diaz-Vela[a], Jui-Hsiang Hung[a], David S. Simmons[b]

[a]The University of Akron, 250 South Forge St. Akron OH 44325

[b]The University of South Florida, 4202 E. Fowler Ave., ENB 118, Tampa, FL 33620

KEYWORDS Glass transition, nanoconfinement, interfacial dynamics, molecular dynamics simulations

ABSTRACT: Near-interface alterations in dynamics and glass formation behavior have been the subject of extensive study for the past two decades, both because of their practical importance and in the hope of revealing underlying correlation lengths underpinning glass transition more generally. Here we employ molecular dynamics simulations of thick films to demonstrate that these effects emerge, for segmental-scale translational dynamics at low temperature, from a temperature-independent rescaling of the local activation barrier. This rescaling manifests as a fractional power law decoupling relationship of local dynamics relative to the bulk, with a transition from a regime of weak decoupling at high temperatures to a regime of strong decoupling at low temperatures. The range of this effect saturates at low temperatures, with 90% of the surface perturbation in the barrier lost over a range of 12 segmental diameters. These findings reduce the phenomenology of T_g nanoconfinement effects to two properties – a position-dependent constant barrier rescaling factor, and an onset timescale – while substantially constraining the predictions required from any theoretical explanation of this phenomenon.

One of the major questions in the understanding of polymer dynamics over the last 20 years has been the nature of apparent alterations in the dynamics, mechanics, and glass formation behavior of polymers and other glass-forming liquids in the nanoscale vicinity of interfaces[1–6]. Evidence suggests that these effects, commonly referred to as "nanoconfinement effects on the glass transition" are in most (but perhaps not all[7]) cases driven by interfacial gradients[1]. The origin of these shifts and even their precise phenomenology remain unresolved questions, which are relevant both to the design of diverse nanostructured materials and the understanding of putative correlation length scales associated with glass formation itself.[8–10] Here we analyze long-time molecular dynamics simulations of thick bead-spring polymer films to show that nanoconfinement effects on segmental-scale translational dynamics take the form of a position-dependent fractional power-law decoupling relationship with bulk dynamics. This finding indicates that nanoconfinement effects are driven by a simple position-dependent rescaling of the activation barrier to relaxation, considerably simplifying the phenomenological picture and providing a profound constraint on theories aiming at its prediction.

We begin by highlighting an apparent discrepancy in the literature that motivates this new picture. Several years ago, our group noted that, if one quantifies in simulation a commonly defined length scale[11–15] ξ_τ over which dynamics near a free surface return to their bulk value, this distance obeys an Adam-Gibbs-like relationship with the segmental translational relaxation time in the film[11]:

$$\log \tau_{film} = A + B\xi_\tau / T \qquad (1)$$

This relation, or nearly equivalent relations, have now been shown to hold at a variety of simulated interfaces [12,13,16]. However, Zhou and Milner recently demonstrated that the same relation holds if one instead employs the *bulk* relaxation time on the left hand side[17]. This poses a quandry. Except for very thin films, ξ_τ is insensitive to film thickness, as it reports on a surface region of perturbed dynamics that exists even at the surfaces of bulk materials. On the other hand, τ_{film} depends on film thickness due to averaging over the very surface gradient reported on by ξ_τ. Equation (1) thus seems to connect a thickness-dependent quantity to at thickness-independent quantity – an apparent contradiction. This set of observations suggests that film dynamics obey a fractional power-law decoupling relationship with bulk dynamics, with a film-thickness dependent decoupling exponent:

$$\langle \tau(h) \rangle \propto \tau_B^{\langle \gamma(h) \rangle} \qquad (2)$$

or

$$\langle \tau(h) \rangle / \tau_B \propto \tau_B^{\langle \varepsilon(h) \rangle} \qquad (3)$$

where γ is the coupling exponent, $\varepsilon = 1 - \gamma$ is the decoupling exponent and brackets indicate overall film values.

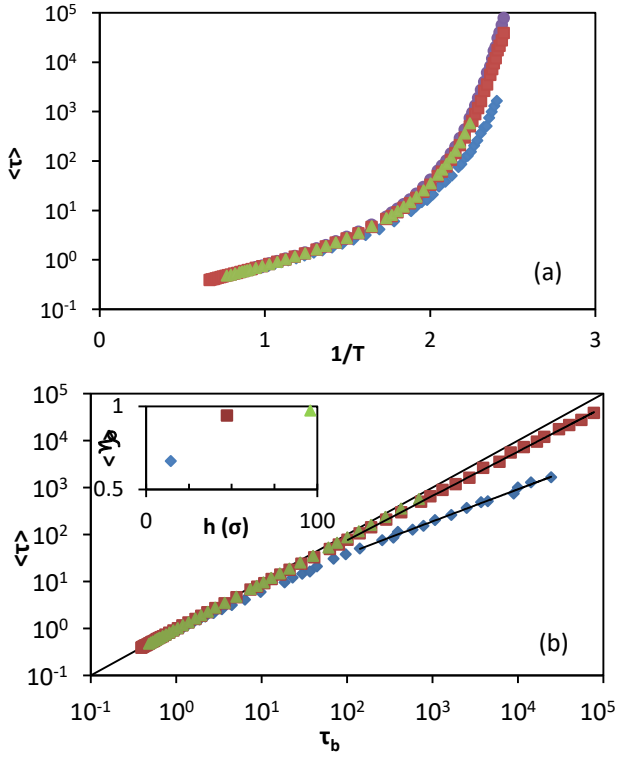

Figure 1. (a) Mean film relaxation times as a function of inverse temperature for bulk system (purple circles) and 15 σ (blue diamonds), 47 σ (red squares), and 96 σ (green trianges) films. (b) Mean film relaxation times plotted vs bulk relaxation times for the same systems. Black lines are fits of data beyond τb = 100 to equation (2). Inset shows the coupling exponent obtained from these fits as a function of film thickness.

Before further discussing the implications of this relation, we employ molecular dynamics simulations of dynamics in model polymer thin films and their bulk analogues to demonstrate that it describes dynamics in freestanding thin films. We study films comprised of 20-bead chains modeled via an attractive bead-spring polymer model[18]. We simulate three thin film systems and their bulk analogues, with thickness of approximately 15 σ, 47 σ, and 97 σ (where σ converts approximately to nm in real units[19–21]). We measure translational segmental relaxation times via the decay of the self-part of the intermediate scattering function at a wavenumber comparable to the first peak of the structure factor, consistent with a common wavenumber convention employed throughout the literature[11,19,22–28]. Resulting mean film relaxation times $\langle\tau\rangle$, which exhibit an enhancement in dynamics with decreasing film thickness, are shown in Figure 1a . See SI for additional methodological details.

If the film relaxation dynamics obey a fractional power-law decoupling relation with bulk dynamics, they must follow a linear relationship with bulk dynamics in the log-log plots suggested by equations (2) and (3). As shown by Figure 1b, this is indeed the case at an overall film level below an onset timescale in the vicinity of 100 τ_{LJ}. The dynamics of layers of thickness 0.875 σ, when similarly plotted against bulk relaxation times in the manner suggested by

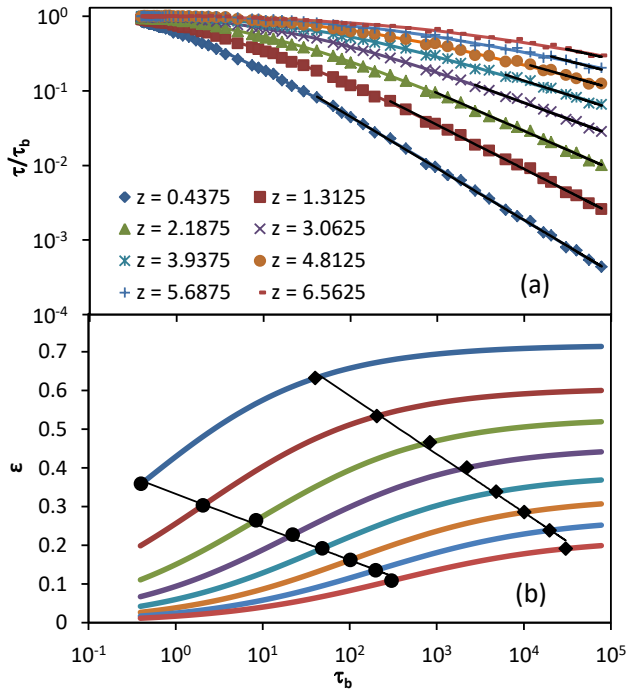

Figure 2. (a) Local film relaxation time normalized by bulk relaxation times at the same temperature, plotted vs bulk relaxation times for layers of mean distance from the interface shown in the inset. Black lines indicate regions of low-temperature linearity Colored lines are fits to equation (7) as described in the text. (b) Decoupling exponents obtained via differentiation of these fits for the same layers of increasing distance from the surface from top to bottom. Circles and triangles denote the crossover midpoint log(τ_c) and plateau onset point log(τ_c)+*w*, respectively, for each layer. Lines are guides to the eye.

equation (3), likewise exhibit a regime of low-temperature linearity indicative of a fractional power law relationship of *local* dynamics with bulk dynamics (Figure 2a).

This low temperature decoupling of film dynamics relative to bulk implies a simple, temperature insensitive rescaling of the effective barrier to relaxation near interfaces. Combining equation (2) with a generalized activation model with a temperature dependent barrier gives

$$\tau(z,T) \propto \exp\left[\frac{\gamma(z)\Delta E_{bulk}(T)}{kT}\right] \quad (4)$$

This, in turn, implies that the activation barrier at a distance *z* from the interface (or the mean barrier in a film of thickness *h*) can be separated into distinct temperature and position dependent factors:

$$\Delta E(z,T) = \gamma(z)\Delta E_{bulk}(T) \quad (5)$$

Here, the first factor *is* the low-temperature nanoconfinement effect; the second factor merely describes the bulk state. In essence, at the level of the underlying barrier, nanoconfinement effects are not temperature dependent beyond the onset temperature. They instead produce a simple temperature-invariant rescaling of the activation

barrier. We note that, since dynamics near T_g do not generally obey an Arrhenius rate law (and certainly do not in this model system), this is a highly nontrivial result. This rescaling of the activation barrier provides a significant constraint on any theoretical explanation of this phenomenon and therefore on the glass transition more generally.

From a practical standpoint, combination of equations (2) and (5) with the Vogel Fulcher Tammann functional form[29,30] indicates that, after accounting for prefactor effects, the film-thickness dependence of T_g reports on the film-thickness dependence of γ:

$$\frac{T_g(h)-T_0^{bulk}}{T_g^{bulk}-T_0^{bulk}}=\gamma(h)\left(1-\frac{\ln\tau_0/\tau_0^{bulk}}{\ln\tau_g/\tau_0^{bulk}}\right)^{-1} \quad (6)$$

where T_0 and τ are the extrapolated divergence temperature and prefactor within the VFT model, τ_g is the conventional timescale of the glass transition, and superscripts of "bulk" denote values in the bulk state. Since equation (5) indicates that $\gamma=\Delta E_{film}/\Delta E_{bulk}$, equation (6) more deeply indicates that, ignoring prefactor effects (which would be expected to become significant if the onset timescale of decoupling approached the 100 second timescale of T_g), the film-thickness dependence of T_g quantifies the rescaling of the activation barrier with decreasing film thickness. This finding suggests that measurements of altered film T_g's, may have a deep connection to fundamental physics.

Studies over the last decade have raised important cautions when connecting whole-film T_g measurements with dynamics[1,31]. Thin-film T_g determinations can be sensitive to the metrology used, with important differences between measurements probing pseudothermodynamics, dynamic relaxation, and high-frequency dynamics. Recently, we have shown that many of these differences can be understood based on differences in how these film-average measurements weight over local gradients in dynamics; in other words, these measurements probe different moments of underlying dynamic distributions[15,32,33], a proposition consistent with a larger body of literature[34–39]. It remains possible that underlying relaxation functions probed by these metrologies may themselves be decoupled; further work is needed in this area[31]. However, these findings imply that, if applied at a whole film level and with an intent to make *quantitative* comparisons in particular, these averaging effects must be taken into account when applying equation (6) or other similar relations.

With this in mind, how do these simulation results compare to experiment? While there is considerable variation in the magnitude and range of these effects[1,15,40–48], experimental observation in thin films and in supported films for which the free surface is dominant (as indicated by a drop in T_g) often report an onset length scale in the loose range of 60 nm (with largest ranges reported in the hundreds of nm[47,48]), with T_g suppressions in the range of 10's of percent in the 10-15 nm range[49–55]. As shown by Figure 1b inset, whole film coupling exponents <γ> obtained by fits of this low temperature regime to equation (2) decrease with decreasing film thickness, with a similar onset thickness and

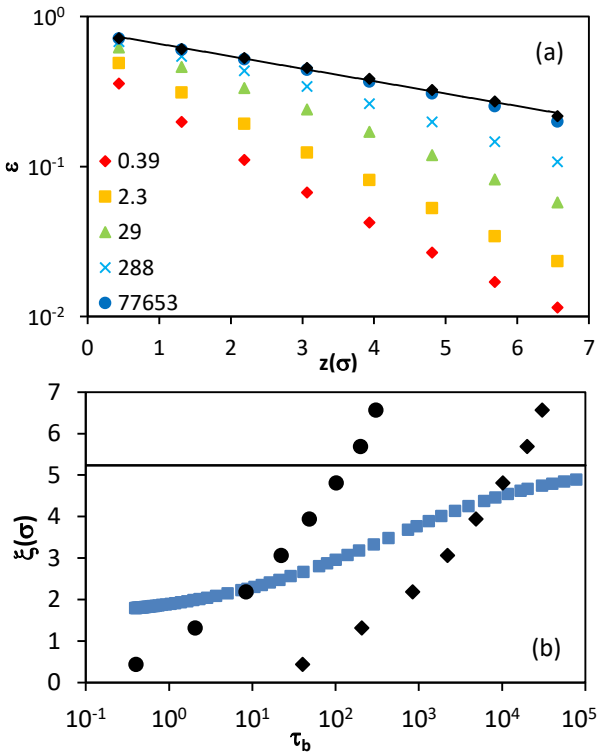

Figure 3. (a) Decoupling exponent vs distance from the surface. Black diamonds denote the limiting low temperature value $\varepsilon_l(z)$; the other points correspond to exponents determined at bulk relaxation times indicated in the legend. The solid line is an exponential fit to the $\varepsilon_l(z)$ data. (b) Decay length scale $\xi_{\Delta F}(\tau_B)$ for the exponential decay of $\varepsilon(z)$ (blue squares), position of the crossover midpoint (black circles) and plateau onset point (black diamonds) vs bulk relaxation time. The solid line indicates the limiting low temperature value of $\xi_{\Delta F}$.

magnitude, as is expected by equation (6). While a quantitative comparison of the magnitudes of these effects would be inappropriate given the complications noted above in comparing dynamic and pseudothermodynamic T_g data, a qualitative agreement of the range and magnitude of these effects indicates that the decoupling scenario described above is reasonably consistent with experimental findings.

Beyond simple agreement with experimental T_g trends in freestanding films, these findings have the potential to explain recent reports that, apparently unlike simulated bead spring models, some experimental glass formers exhibit an apparent onset time scale of nanoconfinement effects in the range of milliseconds[56–58]. We suggest that the onset timescale of thin film decoupling identified above is a plausible candidate for this phenomenon. In particular, the experimental 'fan plots' of Fakhraii and coworkers (see for example figure 5 in Glor et al.[57]) are consistent with what the present viewpoint would anticipate in terms of the temperature dependence of dynamics below this onset point. While this onset is observed at ns timescales in this very minimal polymer model, real chemistries possess more complex potential energy landscapes, potentially delaying the onset of the point at which surface effects appreciably truncate the relaxation barrier. It is furthermore possible

that this time scale depends on the choice of relaxation function. Further research on the dependence of the decoupling onset time on chemistry and relaxation function is evidently needed to explore these possibilities.

The question of the nature and origin of the onset of this decoupling effect is evidently of significant fundamental and practical importance. To better quantify this onset, we employ a fit to a functional form repurposed from its common use[6] to fit thermodynamic data around T_g:

$$\log\frac{\tau}{\tau_b} = w\left(\frac{\varepsilon_l-\varepsilon_h}{2}\right)\ln\left(\cosh\frac{\log\left(\tau_b/\tau_c\right)}{w}\right) + \log\left(\tau_b/\tau_c\right)\left(\frac{\varepsilon_l+\varepsilon_h}{2}\right)+\log c \quad (7)$$

Here, ε_l and ε_h denote the fit values of the low and high temperature limiting decoupling exponents, $2w$ is approximately the width of the crossover between these two values, τ_c is the bulk relaxation time at the midpoint of this crossover, and c is the value of τ/τ_b at this crossover point. We focus on the region $z < 7$ as the deviation from bulk dynamics at greater distances from the interface is too small to allow determination of the fit parameters within reasonable confidence intervals. A free fit to this functional form within the bounds [0,1] for ε_l and ε_h yields $\varepsilon_h \cong 0$ and $w \cong 2$, consistent with a return to bulk like dynamics in the high temperature limit indicating that the crossover exhibits a fixed width of approximately four decades in bulk relaxation time (see SI). In order to reduce fit noise for the remainder of the analysis, we thus enforce $\varepsilon_h = 0$ and $w = 2$. As shown in Figure 2a, the resulting fits describe the data well.

Differentiation of equation (7) with respect to $\log(\tau_b)$ now yields ε as a function of the bulk relaxation time. As shown in Figure 2b, within each layer the decoupling exponent grows upon cooling and approaches a plateau value at low temperature. This plateau corresponds to a low-temperature regime truly obeying the fractional power law decoupling relation encapsulated by equations (2) and (3). In the SI we show the finding of this low temperature plateau is robust to the choice of fitting form and is thus not an artifact of the choice of equation (7). Evidently, these systems indeed exhibit a low temperature fractional power law decoupling relation, with an approximately four decade onset window.

These findings provide a new perspective on the *range* of interface effects on dynamics – an issue of fundamental interest over the last two decades given potential connections to underlying correlation length scales associated with glass formation. Past efforts to quantify this scale have generally focused either on τ or on T_g. The present analysis allows access to information regarding the range of interfacial effects on the underlying *barrier height*, which fundamentally underpins both of these derived quantities. The data in Figure 2 point to *two* underlying types of interfacial range associated with these effects.

First, as shown by Figure 3a, the low temperature barrier $\varepsilon_l(z)$, as reflected via the relation $\varepsilon = 1-\Delta E_{film}/\Delta E_{bulk}$, exhibits an exponential decay back to its bulk value with increasing film depth. This finding explains prior observations of approximately double-exponential decay of the relaxation times away from free surfaces[59]. The decay constant $\xi_{\Delta Fo}$ for this exponential is found to be 5.2 σ in this low temperature limit, indicating that 90% of the surface deviation in ΔE is lost by 12 σ. This range is constant at temperatures well below the onset of decoupling, and is reasonably consistent with the 10 – 20 nm range commonly argued for experimental surface T_g gradients. At higher temperatures, the decay form of ε exhibits weak deviations from exponentiality due to the transit of the transition region seen in Figure 2b through the observation region. However, we can extract an apparent relaxation-time dependent lengthscale $\xi_{\Delta F}(\tau_B)$ for decay of the barrier by fitting the ε vs z data over a range of bulk relaxation times to an approximate exponential form. The results of these fits are shown by the blue squares in Figure 3b: $\xi_{\Delta F}(\tau_B)$ increases on cooling and is consistent with an asymptotic approach to the low temperature limiting value of 5.2σ reported above.

Second, at any given bulk relaxation time (or temperature), there is some distance from the surface within which the film has realized the fully developed decoupling behavior reflecting low temperature ε plateau and beyond which it has not. Since the crossover between these two regimes is broad (approximately four decades as discussed above), this is not a sharply-defined transition. As shown in Figure 2b, we define two measures of the location of this transition: a transition midpoint, $\log(\tau_c)$; and a plateau-onset point, $\log(\tau_c)+w$. As shown in Figure 3b, this plateau onset length scale increases without bound with increasing bulk relaxation time, with the thickness ξ_c of the near-surface region in which the low temperature plateau is fully realized growing approximately linearly with timescale at low temperature. At the longest times, this increasing range has little practical effect, since the low-temperature plateau behavior far from the surface is nearly bulk-like in any case as a consequence of the exponential decay of $\xi_{\Delta Fo}$.

Discussion and Conclusions

Our findings resolve the apparent contradiction motivating this work: the success of equation (1) is insensitive to choice of film thickness (or bulk) because the parameter B captures variations in the mean film coupling exponent $\langle\gamma(h)\rangle$ relating film to bulk dynamics within the power law relation given by equation 2. More broadly, these results are consistent with a revised scenario of alterations in segmental-scale translational dynamics near interfaces:

1) Alterations in near-interface dynamics near the glass transition reflect a simple temperature-invariant suppression of the activation barrier to relaxation, corresponding to a factorization of the local free energy into distinct temperature-dependent and position-dependent factors;
2) This behavior is reflected in a fractional power law relationship between near-surface and bulk relaxation times at low temperature;

3) The free energy barrier exhibits an exponential recovery of bulk values over a range on the order of 10 nm;
4) This decoupling (and factorization) behavior exhibits an onset upon cooling from high temperatures, with the onset delayed with increasing depth in the film.

We note that these simulations are constrained to timescales under 1 microsecond, and we therefore cannot exclude the possibility of 'new physics' at longer timescales. However, the picture presented above appears to be qualitatively consistent with experimental and computational findings and it is thus not clear that any such new physics are needed to explain the observations. We additionally note that at extremely high molecular weights, experiments point to significant changes in the phenomenology of these effects in freestanding films[6,53,60]. Because simulations cannot access these molecular weights, we cannot exclude the possibility of different physics in this regime.

These findings thus suggest that the phenomenology of interface effects on segmental-scale translational dynamics can be reduced to two properties: a thickness- or position-dependent decoupling exponent, which rescales the activation barrier; and an onset time scale for this decoupling. We note that, while multiple efforts to quantify and understand nanoconfinement effects have employed temperature shift approaches (for example position-dependent Vogel temperatures[52,61,62] or rheological shift temperatures[57]), those approaches can be shown to correspond to an effective rescaling of the activation barrier that is *both* position and temperature dependent (see SI). Fundamentally, the finding of a simple temperature invariant rescaling of the activation barrier in thin films is nontrivial for non-Arrhenius systems and should be a key test of future theoretical efforts to understand T_g nanoconfinement effects and the glass transition more broadly.

Indeed, Phan and Schweizer recently demonstrated[63] that the Elastically Cooperative Nonlinear Langevin Equation Theory[64,65] of glass formation, when applied to thin films, predicts decoupling behavior consistent with our preliminary reports of this phenomenon[66] and with the phenomenology reported here. Within this framework, nanoconfinement effects emerge from a weakening of particle caging effects near the free surface and a truncation of a longer-ranged collective barrier. Moreover, this theory predicts that the decoupling phenomenon we observe here persists out to macroscopically observable timescales at least on the order of 100 seconds, lending weight to the proposition that this phenomenon may dominate nanoconfinement effects over a large range of timescales. The question of whether any other theoretical framework is capable of predicting this phenomenology now appears to be a crucial one in the effort to narrow the field of potential theories of the glass transition.

Practically, an understanding of the onset condition of decoupling, and its dependence on chemistry has the potential to resolve a number of apparent discrepancies between simulated bead-based systems (which exhibit high-temperature onsets), experimental systems exhibiting onsets in the vicinity of the 100s timescale of T_g, and experimental systems apparently exhibiting a lack of nanoconfinement effects on reorientational dynamics. Extension of these findings to other chemistries should thus be a priority both for validation of these findings and to study chemistry-dependent trends in these parameters. Finally, extension of these findings to other relaxation functions, such as reorientational and viscous relaxation functions, could have the potential to help resolve apparent differences in nanoconfinement effects experimentally observed via these distinct routes[1,67].

ASSOCIATED CONTENT

Supporting Information. Additional methodological details and supporting data and derivations. This material is available free of charge via the Internet at http://pubs.acs.org.

AUTHOR INFORMATION

Corresponding Author

* dssimmons@usf.edu

Author Contributions

The manuscript was written through contributions of all authors. All authors have given approval to the final version of the manuscript.

ACKNOWLEDGMENT

This material is based upon work supported by the National Science Foundation under Grant No. CBET1705738. The authors acknowledge the W.M. Keck Foundation for generous support enabling development of simulation methodologies employed in this work. The authors thank K. Schweizer for valuable discussions surrounding the idea of spatial decoupling in thin films.

REFERENCES

(1) Simmons, D. S. An Emerging Unified View of Dynamic Interphases in Polymers. *Macromol. Chem. Phys.* **2016**, *217*, 137–148.

(2) Cangialosi, D.; Boucher, V. M.; Alegria, A.; Colmenero, J. Physical Aging in Polymers and Polymer Nanocomposites: Recent Results and Open Questions. *Soft Matter* **2013**.

(3) Richert, R. Supercooled Liquid Dynamics: Advances and Challenges. In *Structural Glasses and Supercooled Liquids*; Wolynes, P. G., Lubchenko, V., Eds.; John Wiley & Sons, Inc., 2012; pp 1–30.

(4) McKenna, G. B. Ten (or More) Years of Dynamics in Confinement: Perspectives for 2010. *Eur. Phys. J. Spec. Top.* **2010**, *189*, 285–302.

(5) Roth, C. B.; Dutcher, J. R. Glass Transition and Chain Mobility in Thin Polymer Films. *J. Electroanal. Chem.* **2005**, *584*, 13–22.

(6) Forrest, J. A.; Dalnoki-Veress, K. The Glass Transition in Thin Polymer Films. *Adv. Colloid Interface Sci.* **2001**, *94*, 167–195.

(7) Park, J.-Y.; McKenna, G. B. Size and Confinement Effects on the Glass Transition Behavior of Polystyrene/o-Terphenyl Polymer Solutions. *Phys. Rev. B* **2000**, *61*, 6667–6676.

(8) Adam, G.; Gibbs, J. H. On the Temperature Dependence of Cooperative Relaxation Properties in Glass-Forming Liquids. *J Chem Phys* **1965**, *43*, 139–146.

(9) Cavagna, A. Supercooled Liquids for Pedestrians. *Phys. Rep.-Rev. Sect. Phys. Lett.* **2009**, *476*, 51–124.

(10) Debenedetti, P. G.; Stillinger, F. H. Supercooled Liquids and the Glass Transition. *Nature* **2001**, *410*, 259–267.

(11) Lang, R. J.; Simmons, D. S. Interfacial Dynamic Length Scales in the Glass Transition of a Model Freestanding Polymer Film and Their Connection to Cooperative Motion. *Macromolecules* **2013**, *46*, 9818–9825.

(12) Ruan, D.; Simmons, D. S. Glass Formation near Covalently Grafted Interfaces: Ionomers as a Model Case. *Macromolecules* **2015**, *48*, 2313–2323.

(13) Hanakata, P. Z.; Douglas, J. F.; Starr, F. W. Interfacial Mobility Scale Determines the Scale of Collective Motion and Relaxation Rate in Polymer Films. *Nat. Commun.* **2014**, *5*, 4163.

(14) Hanakata, P. Z.; Douglas, J. F.; Starr, F. W. Local Variation of Fragility and Glass Transition Temperature of Ultra-Thin Supported Polymer Films. *J. Chem. Phys.* **2012**, *137*, 244901.

(15) Mangalara, J. H.; Marvin, M. D.; Wiener, N. R.; Mackura, M. E.; Simmons, D. S. Does Fragility of Glass Formation Determine the Strength of Tg-Nanoconfinement Effects? *J. Chem. Phys. Under Consideration*.

(16) Lee, J.; Mangalara, J. H.; Simmons, D. S. Correspondence between the Rigid Amorphous Fraction and Nanoconfinement Effects on Glass Formation. *J. Polym. Sci. Part B Polym. Phys.* **2017**, *55*, 907–918.

(17) Zhou, Y.; Milner, S. T. Short-Time Dynamics Reveals Tg Suppression in Simulated Polystyrene Thin Films. *Macromolecules* **2017**, *50*, 5599–5610.

(18) Mackura, M. E.; Simmons, D. S. Enhancing Heterogenous Crystallization Resistance in a Bead-Spring Polymer Model by Modifying Bond Length. *J. Polym. Sci. Part B Polym. Phys.* **2014**, *52*, 134–140.

(19) Baschnagel, J.; Varnik, F. Computer Simulations of Supercooled Polymer Melts in the Bulk and in Confined Geometry. *J. Phys. Condens. Matter* **2005**, *17*, R851–R953.

(20) Kremer, K.; Grest, G. S. Dynamics of Entangled Linear Polymer Melts - a Molecular-Dynamics Simulation. *J. Chem. Phys.* **1990**, *92*, 5057–5086.

(21) Slimani, M. Z.; Moreno, A. J.; Colmenero, J. Heterogeneity of the Segmental Dynamics in Lamellar Phases of Diblock Copolymers. *Macromolecules* **2011**, *44*, 6952–6961.

(22) Betancourt, B. A. P.; Hanakata, P. Z.; Starr, F. W.; Douglas, J. F. Quantitative Relations between Cooperative Motion, Emergent Elasticity, and Free Volume in Model Glass-Forming Polymer Materials. *Proc. Natl. Acad. Sci.* **2015**, *112*, 2966–2971.

(23) Starr, F. W.; Douglas, J. F.; Sastry, S. The Relationship of Dynamical Heterogeneity to the Adam-Gibbs and Random First-Order Transition Theories of Glass Formation. *J. Chem. Phys.* **2013**, *138*, 12A541-12A541-18.

(24) Starr, F. W.; Sciortino, F.; Stanley, H. E. Dynamics of Simulated Water under Pressure. *Phys. Rev. E* **1999**, *60*, 6757–6768.

(25) Simmons, D. S.; Douglas, J. F. Nature and Interrelations of Fast Dynamic Properties in a Coarse-Grained Glass-Forming Polymer Melt. *Soft Matter* **2011**, *7*, 11010–11020.

(26) Cheng, Y.; Yang, J.; Hung, J.-H.; Patra, T. K.; Simmons, D. S. Design Rules for Highly Conductive Polymeric Ionic Liquids from Molecular Dynamics Simulations. *Macromolecules* **2018**, *51*, 6630–6644.

(27) Hsu, D. D.; Xia, W.; Song, J.; Keten, S. Glass-Transition and Side-Chain Dynamics in Thin Films: Explaining Dissimilar Free Surface Effects for Polystyrene vs Poly(Methyl Methacrylate). *ACS Macro Lett.* **2016**, *5*, 481–486.

(28) Shavit, A.; Riggleman, R. A. Influence of Backbone Rigidity on Nanoscale Confinement Effects in Model Glass-Forming Polymers. *Macromolecules* **2013**, *46*, 5044–5052.

(29) Vogel, H. Das Temperatur-Abhängigkeitsgesetz Der Viskosität von Flüssigkeiten. *Phys Zeit* **1921**, *22*, 645–646.

(30) Fulcher, G. S. Analysis of Recent Measurements of the Viscosity of Glasses. *J Am Ceram Soc* **1925**, *8*, 339.

(31) Napolitano, S.; Glynos, E.; Tito, N. B. Glass Transition of Polymers in Bulk, Confined Geometries, and near Interfaces. *Rep. Prog. Phys.* **2017**, *80*, 036602.

(32) Mangalara, J. H.; Mackura, M. E.; Marvin, M. D.; Simmons, D. S. The Relationship between Dynamic and Pseudo-Thermodynamic Measures of the Glass Transition Temperature in Nanostructured Materials. *J. Chem. Phys.* **2017**, *146*, 203316.

(33) Ye, C.; Weiner, C. G.; Tyagi, M.; Uhrig, D.; Orski, S. V.; Soles, C. L.; Vogt, B. D.; Simmons, D. S. Understanding the Decreased Segmental Dynamics of Supported Thin Polymer Films Reported by Incoherent Neutron Scattering. *Macromolecules* **2015**, *48*, 801–808.

(34) Forrest, J. A.; Dalnoki-Veress, K. When Does a Glass Transition Temperature Not Signify a Glass Transition? *ACS Macro Lett.* **2014**, *3*, 310–314.

(35) Mirigian, S.; Schweizer, K. S. Theory of Activated Glassy Relaxation, Mobility Gradients, Surface Diffusion, and Vitrification in Free Standing Thin Films. *J. Chem. Phys.* **2015**, *143*, 244705.

(36) Lipson, J. E. G.; Milner, S. T. Local and Average Glass Transitions in Polymer Thin Films. *Macromolecules* **2010**, *43*, 9874–9880.

(37) Pye, J. E.; Rohald, K. A.; Baker, E. A.; Roth, C. B. Physical Aging in Ultrathin Polystyrene Films: Evidence of a Gradient in Dynamics at the Free Surface and Its Connection to the Glass Transition Temperature Reductions. *Macromolecules* **2010**, *43*, 8296–8303.

(38) Rotella, C.; Wübbenhorst, M.; Napolitano, S. Probing Interfacial Mobility Profiles via the Impact of Nanoscopic Confinement on the Strength of the Dynamic Glass Transition. *Soft Matter* **2011**, *7*, 5260–5266.

(39) Kim, S.; Hewlett, S. A.; Roth, C. B.; Torkelson, J. M. Confinement Effects on Glass Transition Temperature, Transition Breadth, and Expansivity: Comparison of Ellipsometry and Fluorescence Measurements on Polystyrene Films. *Eur. Phys. J. E* **2009**, *30*, 83–92.

(40) Fryer, D. S.; Peters, R. D.; Kim, E. J.; Tomaszewski, J. E.; Nealey, P. F.; White, C. C.; Wu, W. L. Dependence of the Glass Transition Temperature of Polymer Films on Interfacial Energy and Thickness. *Macromolecules* **2001**, *34*, 5627.

(41) Priestley, R. D.; Mundra, M. K.; Barnett, N. J.; Broadbelt, L. J.; Torkelson, J. M. Effects of Nanoscale Confinement and Interfaces on the Glass Transition Temperatures of a Series of Poly(n-Methacrylate) Films. *Aust. J. Chem.* **2007**, *60*, 765–771.

(42) Lang, R. J.; Merling, W. L.; Simmons, D. S. Combined Dependence of Nanoconfined Tg on Interfacial Energy and Softness of Confinement. *ACS Macro Lett.* **2014**, *3*, 758–762.

(43) Merling, W. L.; Mileski, J. B.; Douglas, J. F.; Simmons, D. S. The Glass Transition of a Single Macromolecule. *Macromolecules* **2016**, *49*, 7597–7604.

(44) Zhang, C.; Guo, Y.; Priestley, R. D. Glass Transition Temperature of Polymer Nanoparticles under Soft and Hard Confinement. *Macromolecules* **2011**, *44*, 4001–4006.

(45) Evans, C. M.; Deng, H.; Jager, W. F.; Torkelson, J. M. Fragility Is a Key Parameter in Determining the Magnitude of Tg-Confinement Effects in Polymer Films. *Macromolecules* **2013**, *46*, 6091–6103.

(46) Torkelson, J. M.; Priestley, R. D.; Rittigstein, P.; Mundra, M. K.; Roth, C. B. Novel Effects of Confinement and Interfaces on the Glass Transition Temperature and Physical Aging in Polymer Films and Nanocomposites. *AIP Conf. Proc.* **2008**, *982*, 192–195.

(47) Baglay, R. R.; Roth, C. B. Communication: Experimentally Determined Profile of Local Glass Transition Temperature across a Glassy-Rubbery Polymer Interface with a Tg Difference of 80 K. *J. Chem. Phys.* **2015**, *143*, 111101.

(48) Evans, C. M.; Kim, S.; Roth, C. B.; Priestley, R. D.; Broadbelt, L. J.; Torkelson, J. M. Role of Neighboring Domains in Determining the Magnitude and Direction of Tg-Confinement Effects in Binary, Immiscible Polymer Systems. *Polymer* **2015**, *80*, 180–187.

(49) Keddie, J. L.; Jones, R. A. L.; Cory, R. A. Size-Dependent Depression of the Glass Transition Temperature in Polymer Films. *Europhys. Lett. EPL* **1994**, *27*, 59–64.

(50) Sharp, J. S.; Teichroeb, J. H.; Forrest, J. A. The Properties of Free Polymer Surfaces and Their Influence on the Glass Transition Temperature of Thin Polystyrene Films. *Eur. Phys. J. E Soft Matter* **2004**, *15*, 473–487.

(51) Ellison, C. J.; Mundra, M. K.; Torkelson, J. M. Impacts of Polystyrene Molecular Weight and Modification to the Repeat Unit Structure on the Glass Transition-Nanoconfinement Effect and the Cooperativity Length Scale. *Macromolecules* **2005**, *38*, 1767–1778.

(52) Yang, Z.; Fujii, Y.; Lee, F. K.; Lam, C.-H.; Tsui, O. K. C. Glass Transition Dynamics and Surface Layer Mobility in Unentangled Polystyrene Films. *Science* **2010**, *328*, 1676–1679.

(53) Alcoutlabi, M.; McKenna, G. B. Effects of Confinement on Material Behaviour at the Nanometre Size Scale. *J. Phys. Condens. Matter* **2005**, *17*, R461–R524.

(54) Koh, Y. P.; McKenna, G. B.; Simon, S. L. Calorimetric Glass Transition Temperature and Absolute Heat Capacity of Polystyrene Ultrathin Films. *J. Polym. Sci. Part B Polym. Phys.* **2006**, *44*, 3518–3527.

(55) Wang, J.; McKenna, G. B. A Novel Temperature-Step Method to Determine the Glass Transition Temperature of Ultrathin Polymer Films by Liquid Dewetting. *J. Polym. Sci. Part B Polym. Phys.* **2013**, *51*, 1343–1349.

(56) Daley, C. R.; Fakhraai, Z.; Ediger, M. D.; Forrest, J. A. Comparing Surface and Bulk Flow of a Molecular Glass Former. *Soft Matter* **2012**, *8*, 2206–2212.

(57) Glor, E. C.; Composto, R. J.; Fakhraai, Z. Glass Transition Dynamics and Fragility of Ultrathin Miscible Polymer Blend Films. *Macromolecules* **2015**, *48*, 6682–6689.

(58) Fakhraai, Z.; Forrest, J. A. Measuring the Surface Dynamics of Glassy Polymers. *Science* **2008**, *319*, 600–604.

(59) Scheidler, P.; Kob, W.; Binder, K. The Relaxation Dynamics of a Confined Glassy Simple Liquid. *Eur. Phys. J. E* **2003**, *12*, 5–9.

(60) Pye, J. E.; Roth, C. B. Two Simultaneous Mechanisms Causing Glass Transition Temperature Reductions in High Molecular Weight Freestanding Polymer Films as Measured by Transmission Ellipsometry. *Phys. Rev. Lett.* **2011**, *107*, 235701.

(61) Napolitano, S.; Lupaşcu, V.; Wübbenhorst, M. Temperature Dependence of the Deviations from Bulk Behavior in Ultrathin Polymer Films. *Macromolecules* **2008**, *41*, 1061–1063.

(62) Chowdhury, M.; Guo, Y.; Wang, Y.; Merling, W. L.; Mangalara, J. H.; Simmons, D. S.; Priestley, R. D. Spatially Distributed Rheological Properties in Confined Polymers by Noncontact Shear. *J. Phys. Chem. Lett.* **2017**, 1229–1234.

(63) Phan, A. D.; Schweizer, K. S. Dynamic Gradients, Mobile Layers, Tg Shifts, Role of Vitrification Criterion, and Inhomogeneous Decoupling in Free-Standing Polymer Films. *Macromolecules* **2018**, *51*, 6063–6075.

(64) Mirigian, S.; Schweizer, K. S. Elastically Cooperative Activated Barrier Hopping Theory of Relaxation in Viscous Fluids. I. General Formulation and Application to Hard Sphere Fluids. *J. Chem. Phys.* **2014**, *140*, 194506.

(65) Mirigian, S.; Schweizer, K. S. Elastically Cooperative Activated Barrier Hopping Theory of Relaxation in Viscous Fluids. II. Thermal Liquids. *J. Chem. Phys.* **2014**, *140*, 194507.

(66) Simmons, D.; Diaz Vela, D.; Hung, J.-H.; Guo, Hao. Scale-Free Interfacial Dynamic Decoupling Drives Free-Surface Effects on the Glass Transition. In *Bulletin of the American Physical Society*; American Physical Society.

(67) Vogt, B. D. Mechanical and Viscoelastic Properties of Confined Amorphous Polymers. *J. Polym. Sci. Part B Polym. Phys.* **2018**, *56*, 9–30.

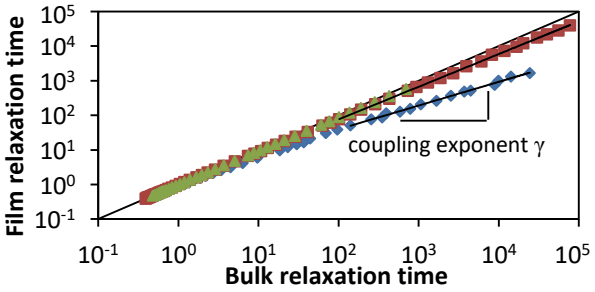
Film relaxation time
Bulk relaxation time
coupling exponent γ
10^5
10^4
10^3
10^2
10^1
10^0
10^-1
10^-1
10^0
10^1
10^2
10^3
10^4
10^5